

SANDIA REPORT

SAND89-1720 • UC-906

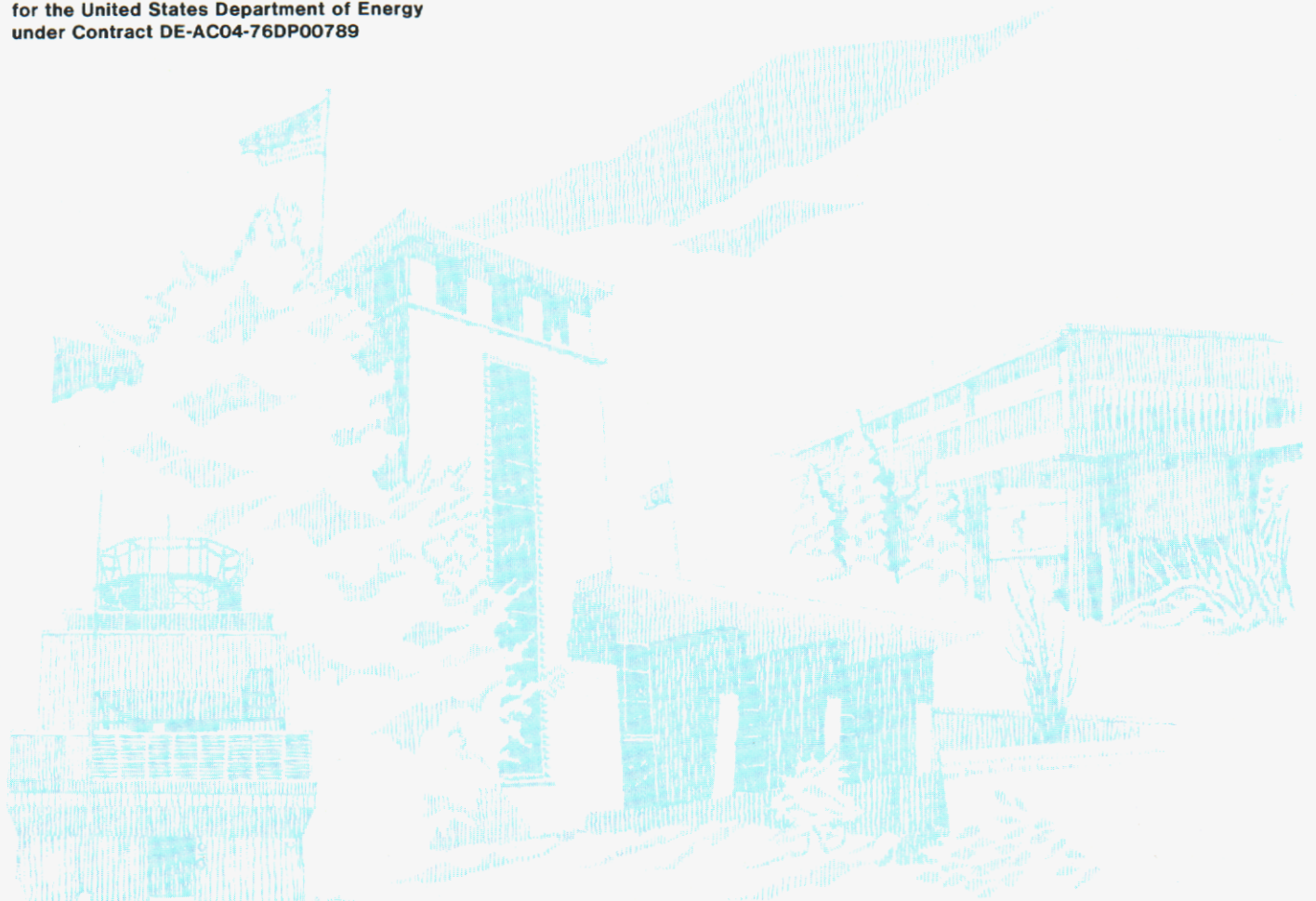
Unlimited Release

Printed October 1989

Gelled Propellant Flow: Boundary Layer Theory for Power-Law Fluids in a Converging Planar Channel

A. M. Kraynik, A. S. Geller, J. H. Glick

Prepared by
Sandia National Laboratories
Albuquerque, New Mexico 87185 and Livermore, California 94550
for the United States Department of Energy
under Contract DE-AC04-76DP00789



Issued by Sandia National Laboratories, operated for the United States Department of Energy by Sandia Corporation.

NOTICE: This report was prepared as an account of work sponsored by an agency of the United States Government. Neither the United States Government nor any agency thereof, nor any of their employees, nor any of their contractors, subcontractors, or their employees, makes any warranty, express or implied, or assumes any legal liability or responsibility for the accuracy, completeness, or usefulness of any information, apparatus, product, or process disclosed, or represents that its use would not infringe privately owned rights. Reference herein to any specific commercial product, process, or service by trade name, trademark, manufacturer, or otherwise, does not necessarily constitute or imply its endorsement, recommendation, or favoring by the United States Government, any agency thereof or any of their contractors or subcontractors. The views and opinions expressed herein do not necessarily state or reflect those of the United States Government, any agency thereof or any of their contractors or subcontractors.

Printed in the United States of America. This report has been reproduced directly from the best available copy.

Available to DOE and DOE contractors from
Office of Scientific and Technical Information
PO Box 62
Oak Ridge, TN 37831

Prices available from (615) 576-8401, FTS 626-8401

Available to the public from
National Technical Information Service
US Department of Commerce
5285 Port Royal Rd
Springfield, VA 22161

NTIS price codes
Printed copy: A02
Microfiche copy: A01

Distribution
UC-906

SAND89-1720
Unlimited Release

Gelled Propellant Flow: Boundary Layer Theory for Power-Law Fluids in a Converging Planar Channel*

A. M. Kraynik, A. S. Geller, and J. H. Glick
Fluid and Thermal Sciences Department

Sandia National Laboratories
Albuquerque, NM 87185

Abstract

A boundary layer theory for the flow of power-law fluids in a converging planar channel has been developed. This theory suggests a Reynolds number for such flows, and following numerical integration, a boundary layer thickness. This boundary layer thickness has been used in the generation of a finite element mesh for the finite element code FIDAP. FIDAP was then used to simulate the flow of power-law fluids through a converging channel. Comparison of the analytic and finite element results shows the two to be in very good agreement in regions where entrance and exit effects (not considered in the boundary layer theory) can be neglected.

*This work was performed at Sandia National Laboratories, supported by the U.S. Department of Energy under Contract DE-AC04-76DP00789.

Contents

1 Introduction	1
2 Boundary Layer Theory	2
3 Numerical Simulation	4
4 Conclusions	7
5 References	8

List of Figures

1	Schematic of cavitating venturi	9
2	Boundary layer solution for flow through a contraction	10
3	Wall shear stress	11
4	Schematic of two-dimensional channel	12
5	Finite element mesh based on boundary layer analysis	13
6	Expanded view of mesh in entrance region	14
7	Streamlines for flow through converging channel	15
8	Comparison of analytic and numerical results for flow in the boundary layer	16

List of Tables

1	Reynolds number as a function of power-law index and entrance velocity	7
---	--	---

INTENTIONALLY LEFT BLANK.

1 Introduction

The design of propulsion systems that use gelled propellants requires an understanding of gel rheology and its effect on high-speed flows in complex geometries. The current design strategy to maintain optimum fuel/oxidizer mixing ratio is based on the assumption that flow behavior of both the fuel and oxidizer gels is identical. TRW is measuring the viscosity function of hypergolic gelled propellants developed by MICOM (Allan, 1987). The gelled fuel, MICOM GEL, contains monomethylhydrazine (MMH), aluminum filler particles, and a polymeric gellant. The gelled oxidizer, IRFNA GEL, contains inhibited red fuming nitric acid (IRFNA), suspended lithium nitrate particles, and fumed silica. The TRW measurements have not been completed but indicate that these fluids are highly shear thinning with power-law exponents $n \approx 0.3$. Furthermore, the existing data do not show evidence of wall slip.

The current TRW engine design for gels uses a cavitating venturi valve in each propellant stream (Figure 1). These valves are major engine components that provide pressure isolation as well as flow rate control. The desired operating characteristics of cavitating venturis depend on dominant inertial effects associated with axial flow through axisymmetric annular regions of continuously varying gap. Current design methods are based on Newtonian fluid mechanics, so it is important to undertake numerical simulations of non-Newtonian flows in complex geometries to design for gels.

We have developed a boundary layer theory for the flow of power-law fluids in converging planar channels. This analysis provides estimates of boundary layer thickness, which can be used to optimize mesh generation for finite element numerical simulations. The numerical computations can then be compared with the similarity solutions. This analysis extends the classical Newtonian solution of Pohlhausen, which is discussed by Schlichting (1979).

2 Boundary Layer Theory

In a power-law fluid, the relation between shear rate, $\dot{\gamma}$, and shear stress, τ , is given by the relation:

$$\tau = m|\dot{\gamma}|^{n-1}\dot{\gamma},$$

where n is the power-law index and m is the power-law coefficient, analogous to the Newtonian viscosity. The boundary layer equation for a power-law fluid is then:

$$u \frac{\partial u}{\partial x} + v \frac{\partial u}{\partial y} = U \frac{dU}{dx} + \frac{m}{\rho} \frac{\partial}{\partial y} \left[\left| \frac{\partial u}{\partial y} \right|^{n-1} \frac{\partial u}{\partial y} \right]. \quad (1)$$

For flow in a converging planar channel, the potential flow velocity $U = -K/x$, where K is a flow rate parameter; ρ is the fluid density. The coordinate system origin is at the sink point. Choosing

$$u = U f'(\eta) \quad \text{and} \quad \eta = yx^{-1} Re_x^{1/(1+n)},$$

where $Re_x = \rho x^n |U|^{2-n}/m$, the continuity equation and (1) are transformed into the ordinary differential equation

$$\frac{d}{d\eta} (f f'' |f''|^{n-1}) + 1 - f'^2 + \frac{2(n-1)}{n+1} f f'' = 0, \quad (2)$$

with boundary conditions:

$$f(0) = f'(0) = 0 \quad \text{and} \quad f'(\infty) = 1.$$

For a Newtonian fluid, $n = 1$, and Equation (2) becomes

$$f''' + 1 - f'^2 = 0, \quad (3)$$

where $\eta = yx^{-1} Re_x^{1/2}$ and $Re_x = K\rho/\mu$. Pohlhausen's solution for the velocity is:

$$f' = u/U = 3 \tanh^2 (2^{-1/2} \eta + \tanh^{-1}(2/3)^{1/2}) - 2,$$

and the corresponding boundary layer thickness is given by

$$\delta \sim x Re_x^{-1/2} \sim x K^{-1/2}.$$

The boundary layer thickness for a power-law fluid is evident from the similarity variables and is given by

$$\delta = F(n) x Re_x^{-1/(1+n)} \sim x^{(3-n)/(1+n)} K^{(n-2)/(1+n)}.$$

The function $F(n)$ is determined by solving Equation (2). For a highly shear thinning power-law fluid, $\delta \sim x^3 K^{-2}$ for $n \rightarrow 0$. The scaling with distance and flow rate is much stronger than the Newtonian scaling.

It was necessary to integrate Equation (2) numerically for $n \neq 1$. We used the program SUPORQ from the SLATEC Library (Haskell, 1986). Following established procedure for the Newtonian problem, the far-field boundary condition was replaced by $f'(\eta_\infty) = 1$, for some large η_∞ , e.g. $\eta_\infty = 10$. This appeared to be satisfactory for n not too different than 1, but led to severe "kinks" in the solution for f' at η_∞ when n was small. These discontinuities in slope could be reduced by increasing η_∞ for small n , but this required such large values of η_∞ for $n < 0.2$ that numerical instabilities developed.

The solution behavior for small n is important because gelled propellants and other non-Newtonian materials under consideration in weapon applications are highly shear thinning. The numerical difficulties stem from the asymptotic behavior of f' for large η . The analytical solution for a Newtonian fluid gives

$$f' \sim 1 - Ce^{-\sqrt{2}\eta} \quad \text{as } \eta \rightarrow \infty,$$

where C is a known constant. With the assistance of Romero (1989), we obtained the asymptotics for $n \neq 1$, which are very different:

$$f' \sim 1 - a(n) x^{-N} [\log(x) + \dots]^{1/(1-n)}, \quad (4)$$

where $a(n) = n^{1/(1-n)} N^N$ and $N = (1+n)/(1-n)$.

The slow algebraic approach to free stream conditions for a highly shear thinning fluid is in sharp contrast with the exponential behavior for Newtonian fluids. We have obtained higher order corrections to Equation (4). Knowing the asymptotics, it seemed reasonable to solve our problem by using the program D02HBF from the NAG (Numerical Algorithms Group, 1981) library. This code integrates a system of differential equations subject

to given boundary conditions and given asymptotic forms. The code did not prove useful because of numerical convergence problems associated with the slow decay indicated by Equation (4).

We were able to obtain accurate solutions by using the mixed boundary condition capability of SUPORQ. The asymptotic solution (4) is consistent with

$$f' \sim 1 - \frac{1-n}{1+n} \eta f''.$$

Instead of forcing f' to 1, this equation is used for the boundary condition at η_∞ . Solution accuracy was demonstrated by varying η_∞ . Representative solutions for $f'(\eta; n)$ are shown in Figure 2. We have used these results to compute the boundary layer thickness function $F(n)$ and have also computed $f''(0; n)$, which determines the wall shear stress and is shown in Figure 3.

3 Numerical Simulation

To test the use of the power-law boundary layer solution in mesh generation, a two-dimensional channel (similar to the converging channel flow for which the analytic solution was derived) is used. This channel consists of an entrance region with constant thickness followed by a converging section. The channel is illustrated in Figure 4 with the flow from left to right. The upper wall is a no-slip surface, the lower boundary defines a plane of symmetry, and the entrance and exit are tractionless. The flow at the entrance is steady, unidirectional flow with velocity U_{inf} .

One result of the boundary layer analysis is a definition of a Reynolds number for power law fluids in this type of flow given by $Re_x = \rho x^n |U|^{2-n} / m$. Re_x is evaluated using parameters corresponding to the MICOM GEL, $\rho = 1.0 \text{ gm/cm}^3$ is the fluid density, n is the power-law index for the fluid, and $m = 0.01$ is the power-law coefficient. The distance along the upper surface from the point of intersection of the upper wall and the plane of symmetry in the converging channel is given by x . The boundary layer analysis also defines a similarity variable $\eta = (y/x) Re_x^{1/(1+n)}$, where y is the distance from

a point in the fluid to the plane of the sloping upper surface. Thus, as the Reynolds number of the flow or n increases, the thickness of the boundary layer decreases.

Using the results of the numerical integration of Equation (2), a value of $\eta = 4$ was chosen to define the end of the boundary layer for the purpose of mesh generation. Given values for η , ρ , and m , the distance from the upper plate to the outer edge of the boundary layer can be calculated. Using $\eta = 4$ the thickness of the boundary layer is $\delta = 4xRe_x^{-1/1+n}$. The boundary layer thickness was calculated for both the entrance and exit end of the converging region. With this information, a mesh was generated which concentrates nodes parallel to the sloping wall in a domain equal to 3δ (as defined by $\eta = 4$) from the upper surface while using a relatively coarse mesh in the outer region. The factor of three was chosen to correct for the choice of $\eta = 4$ as the end of the boundary layer. An example of such a mesh is shown in Figure 5 for the case $n = 0.35$. The extremely fine grid can be seen near the upper surface, and the contraction of the boundary layer as x decreases along the plate length is reflected in a narrowing of the fine grid region. The grid used in the outer domain allows a significant saving of computer resources, though in order to be compatible with the mesh in the boundary layer, the grid is not as coarse as it could be. Figure 6 shows an expanded view of the grid at the entrance to the converging section. This illustrates the alignment of the grid with the converging wall.

Although basing the boundary layer thickness on a large value of η is reasonable for moderate values of n , as n becomes small, the velocity in the boundary layer approaches the free stream velocity extremely slowly. The behavior of the solution for $n = 0.1$ in Figure 2 illustrates this. The velocity for this case rapidly approaches the outer velocity in the region $0 < \eta < 1.0$ but changes less than 10% for $1.0 < \eta < 5.0$. For this case, rather than being a conservative choice, choosing $\eta = 12$ as the outer edge of the boundary layer might not extend the fine grid far enough. In fact, to model fluids with these extremely small power-law indices, three levels of grid refinement might be necessary: a very fine grid for low values of η in the narrow region in which the flow reaches a value of dimensionless velocity $f' \sim 0.8$, this region would have thickness $O(f''(0)^{-1})$. This region would be followed by a larger

intermediate region which captures the slow approach of the boundary layer velocity to the outer flow, and finally, the coarse outer region. As additional flows for fluids with $n = 0.3$ are modeled, convergence problems may develop. If this occurs, a likely reason may be that the choice of $\eta = 4$ was not able to capture the full boundary layer in these flows. If this problem does arise, it will be necessary to re-examine our definition of the boundary layer thickness.

Using meshes generated to concentrate nodes in the boundary layer, $\eta < 4$, calculations were carried out with the finite element code FIDAP (Fluid Dynamics International, 1987) for several values of U_{inf} and n . Table 1 shows the power-law indices, velocities, and Reynolds numbers for which calculations were performed. The smallest power law index used was $n = 0.3$ (equal to that which describes the actual gelled propellants) yielding a Reynolds number based on the length of the converging region of 2100. The maximum Reynolds number for which we have generated a solution is 10,000. Figure 7 shows the streamlines for the flow of a power-law fluid with $n = 0.6$ and $U_{inf} = 7.5$ cm/s for which $Re = 6700$. The narrowing of the boundary layer along the sloping upper surface can be seen in the streamline lying nearest the upper boundary.

n/U	10.0	7.5	4.0
1.0	10,000	-	4000
0.8	10,000	7000	3300
0.6	-	6700	2800
0.5	-	6500	2500
0.45	-	6400	2400
0.4	-	-	2300
0.35	-	-	2200
0.3	-	-	2100

Table 1: Reynolds number as a function of power-law index and entrance velocity

4 Conclusions

The results from the finite element calculation are compared with the analytic solution for the flow in the boundary layer in Figure 8. The variable y_{out} represents the distance from the symmetry plane of a node at the channel exit. Lines of constant y_{out} are those following the mesh from this point (i.e., lines parallel to the down-sloping wall in Figure 6). The plot shows that except for points lying near the entrance or exit of the converging region (for which the boundary layer solution does not apply) the numerical and analytic results are in very good agreement. Having demonstrated that the use of the boundary layer theory for power-law fluids allows us to optimize the mesh in converging flows, we will now begin to apply this method to calculation of flows in actual cavitating venturi geometries.

5 References

Allan, B., Private Communication, MICOM, Huntsville, AL, 1987.

Fluid Dynamics International Co., *FIDAP Users Manual*, Evanston, IL, 1987.

Haskell, K., Slatec On-Line Documentation, Sandia National Laboratories, Albuquerque, NM, 1986.

Numerical Algorithms Group, *NAG Fortran Library Manual*, Downers Grove, IL, 1981.

Romero, L., Private Communication, Sandia National Laboratories, Albuquerque, NM, 1989.

Schlichting, H., *Boundary Layer Theory*, McGraw-Hill Book Company, New York, 1979.

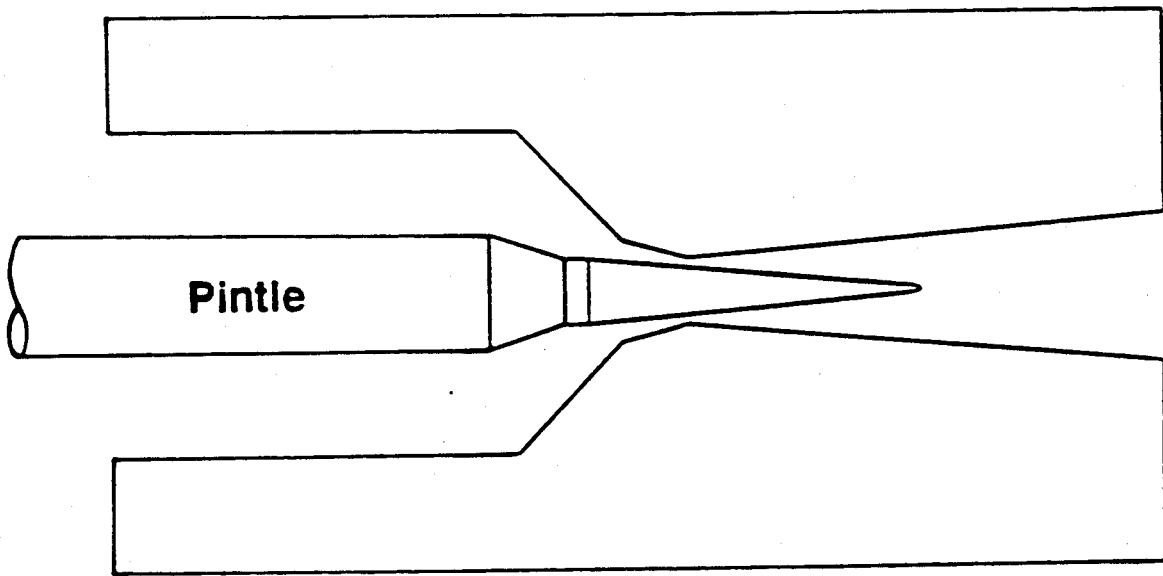


Figure 1: Schematic of cavitating venturi

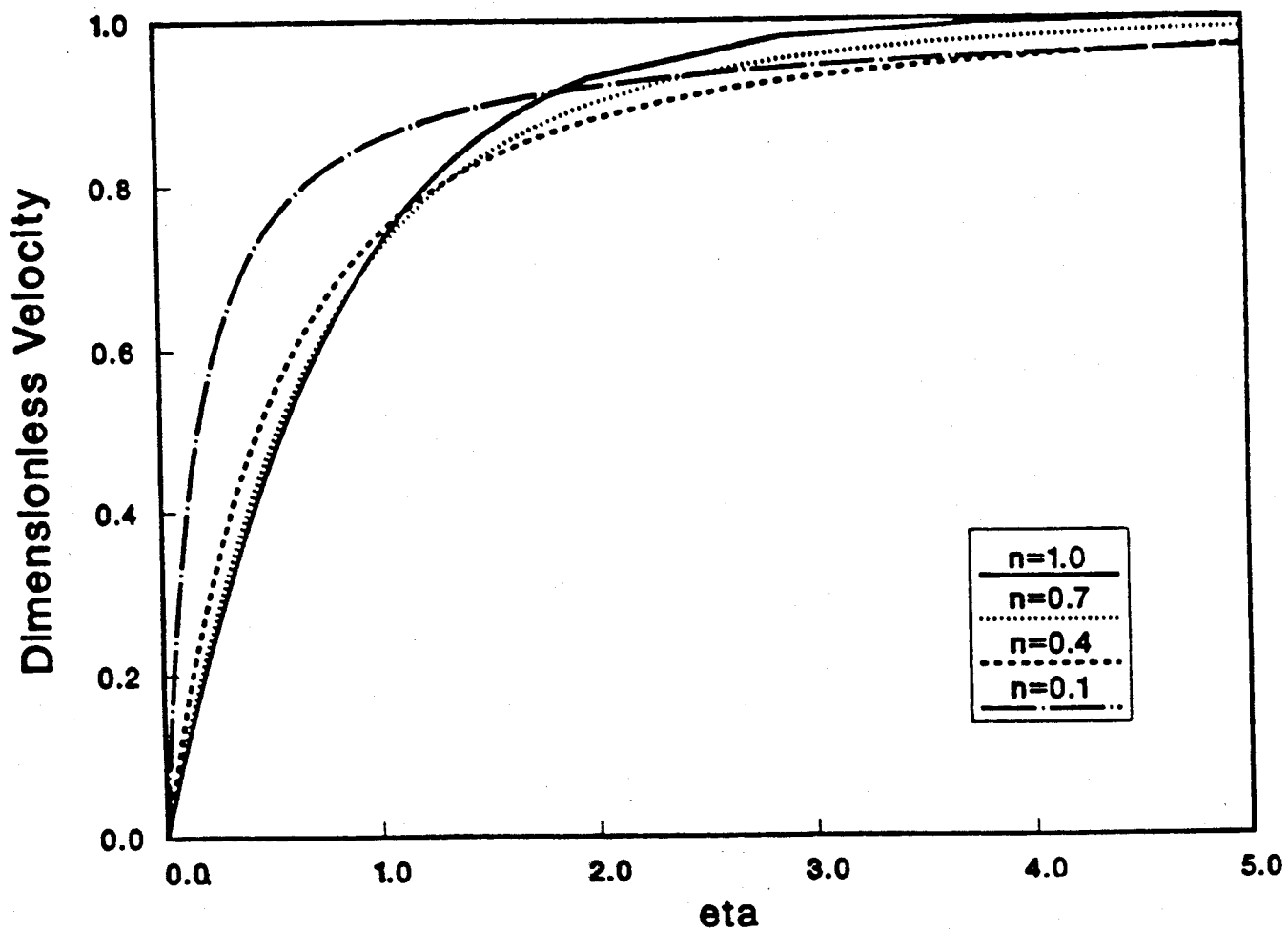


Figure 2: Boundary layer solution for flow through a contraction

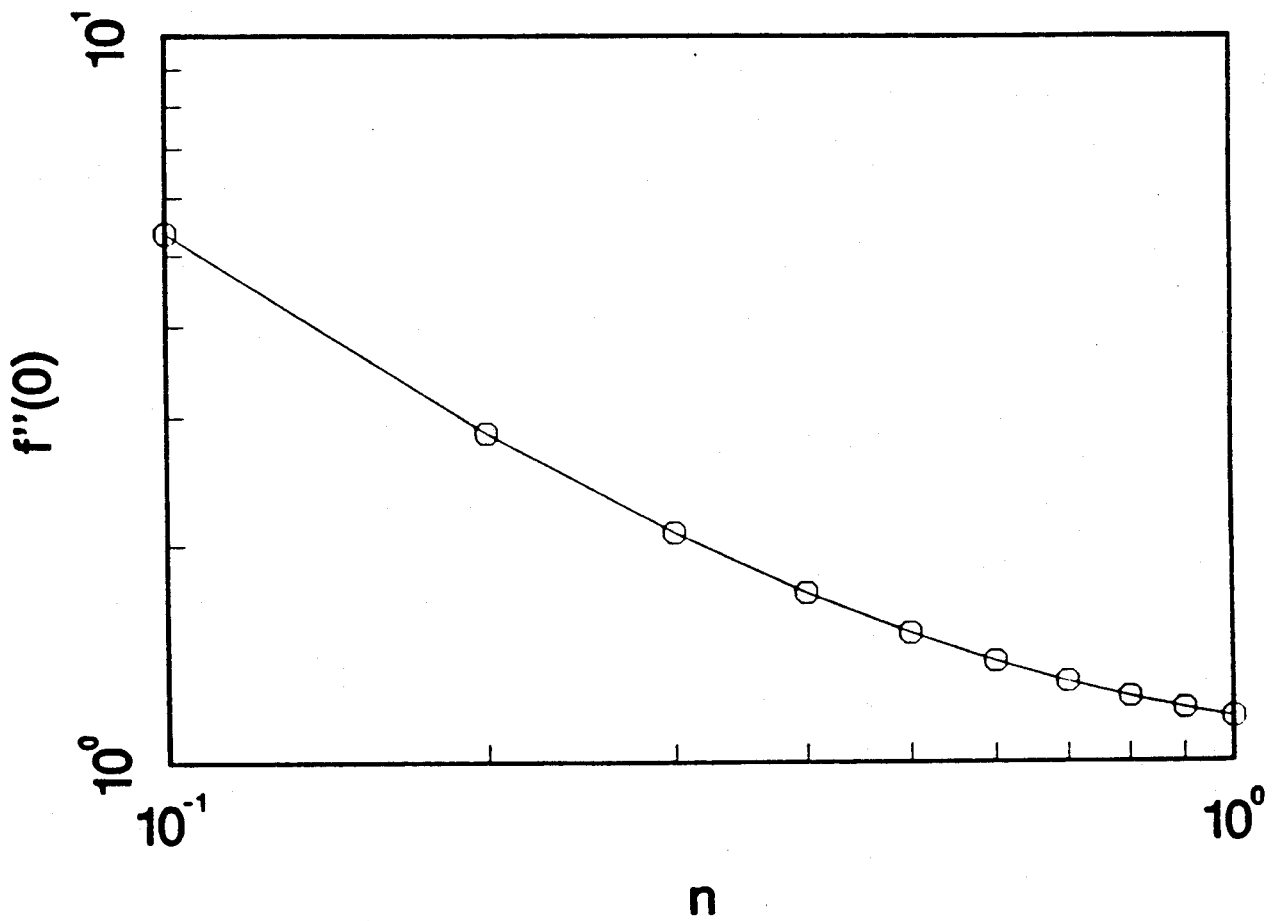


Figure 3: Wall shear stress

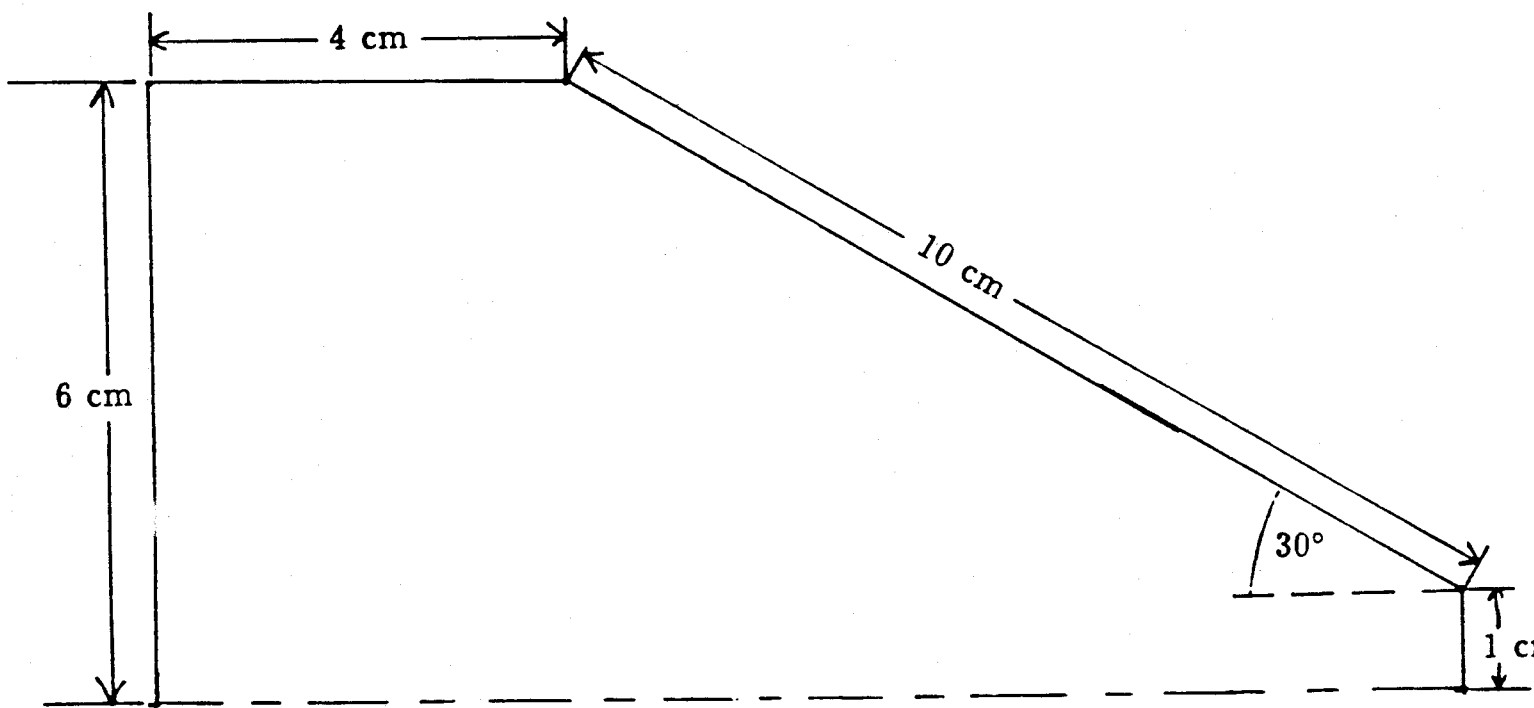


Figure 4: Schematic of two-dimensional channel

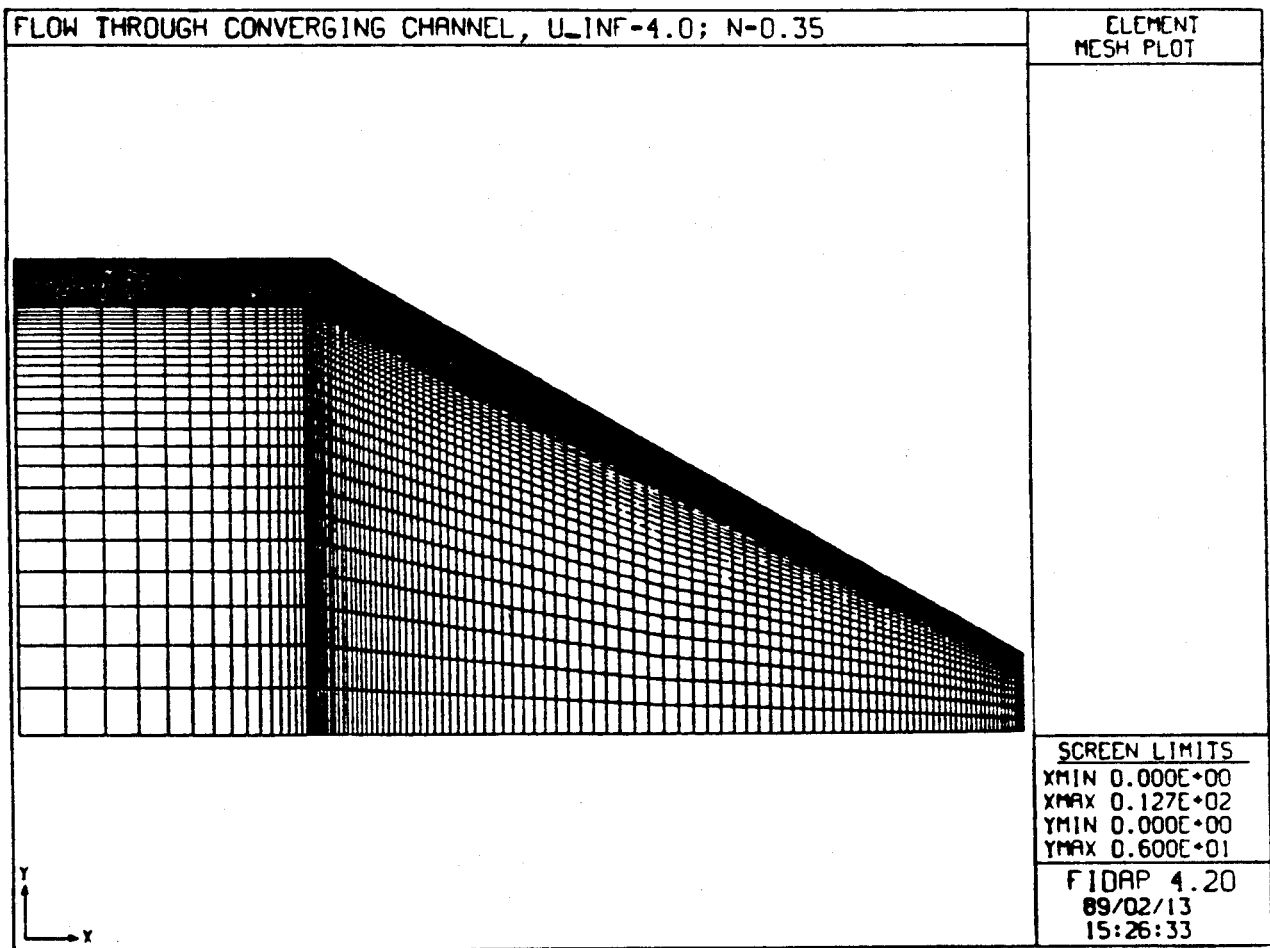


Figure 5: Finite element mesh based on boundary layer analysis

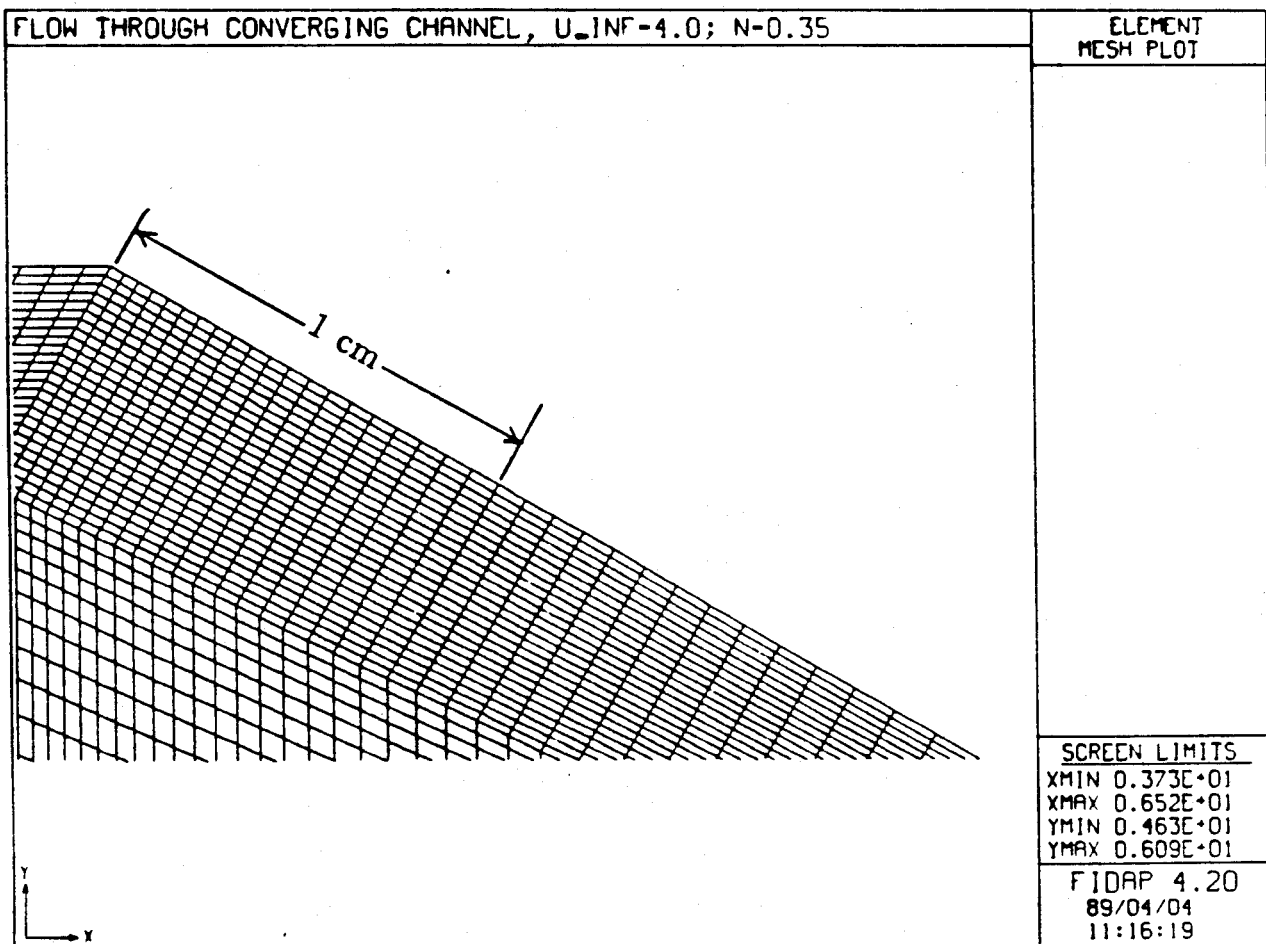


Figure 6: Expanded view of mesh in entrance region

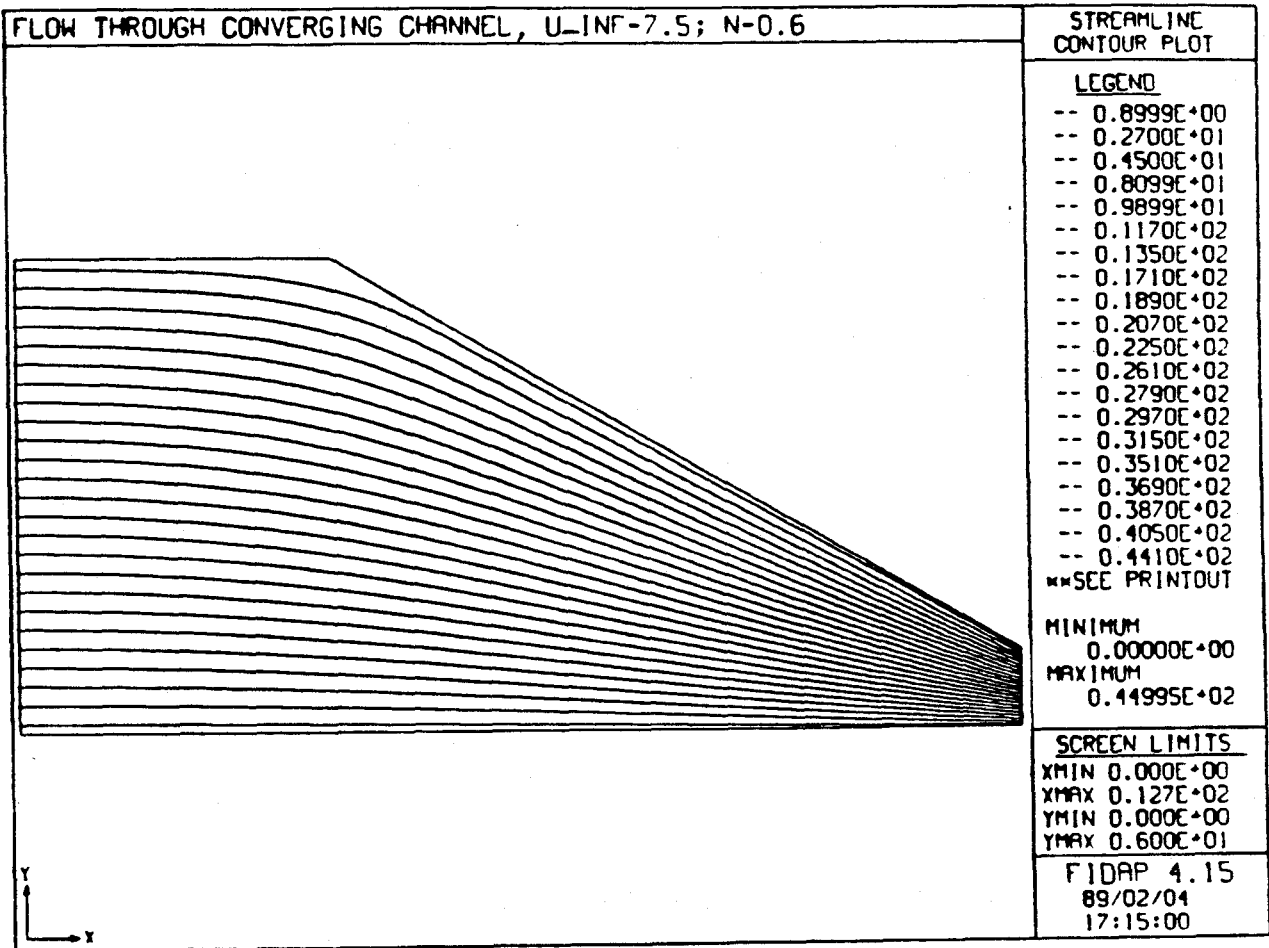


Figure 7: Streamlines for flow through converging channel

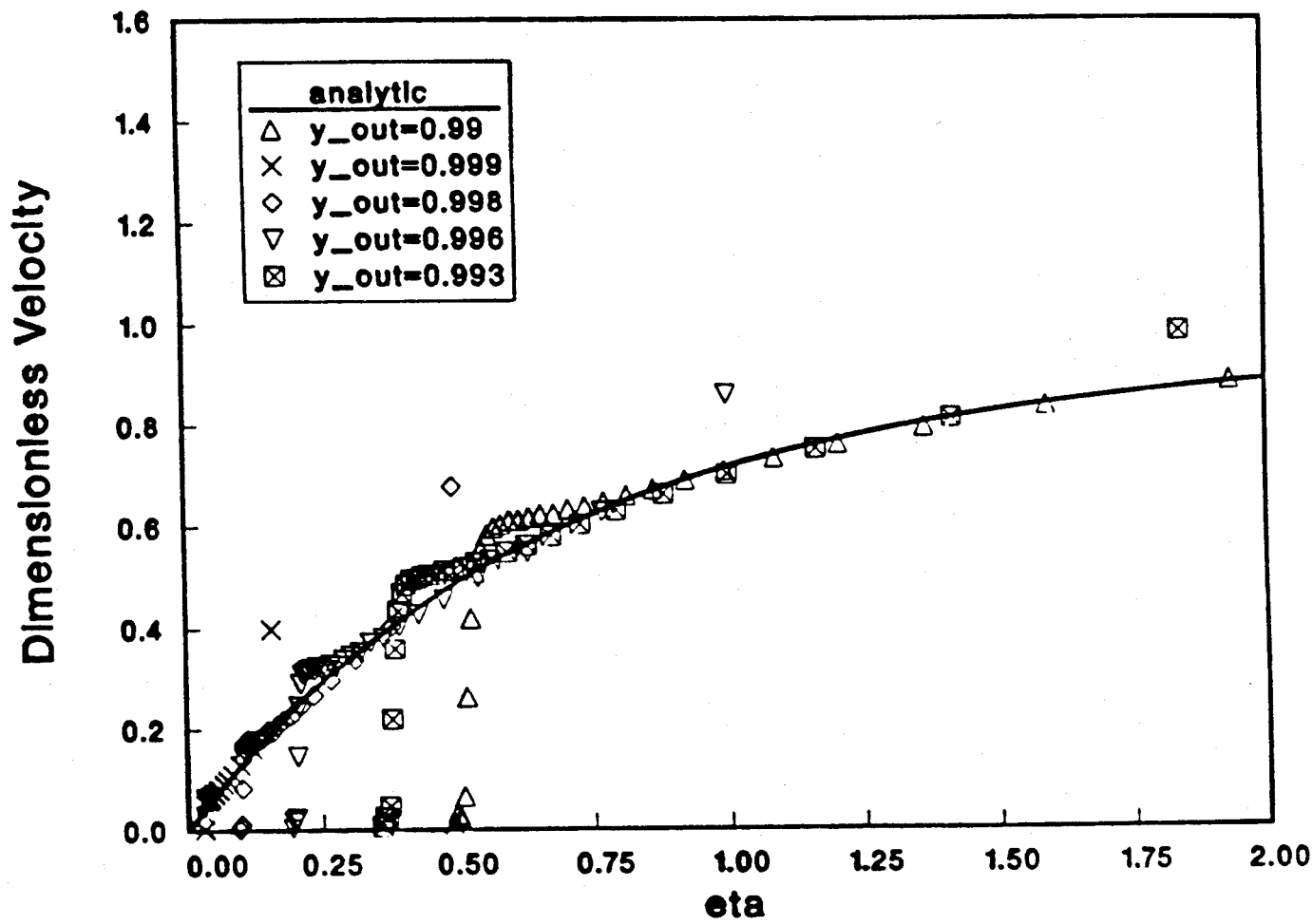


Figure 8: Comparison of analytic and numerical results for flow in the boundary layer

Distribution:

UC-906

External Distribution:

US Army Missile Command

ATTN: Barry Allen

Propulsion Directorate

Redstone Arsenal

Alabama, 35899-5249

US Army Ballistic Research Laboratory

ATTN: SLCBR-TB-EE (Robert Frey)

Aberdeen Proving Ground, MD 21005-5066

Commander

ATTN: Code 389 (Tom Boggs)

Naval Weapons Center

China Lake, CA 93555-6001

Commander

US Army Armaments Research, Development, and Engineering Center

ATTN: SMCAR-AEE-WW (Barry Fishburn)

Dover, NJ 07801-5001

Commander

US Army Missile Command (2)

ATTN: AMSI-RD-PR (Walter Wharton)

(L. B. Thorn)

Redstone Arsenal, AL 35898-5254

AFATL/MNE

ATTN: Gary Parsons

Eglin AFB, FL 32542-5434

Commander (2)
ATTN: Code 101 (Richard Bernecker)
Code 101 (Les Roslund)
Naval Surface Warfare Center, White Oak
Silver Spring, MD 20903-5000

Commander
US Army Belvoir Research, Development, and Engineering Center
ATTN: STRBE-NMC (Pam Jacobs)
Fort Belvoir, VA 22060

Director
US Army Ballistic Research Laboratory
ATTN: SLCBR-IC-I (Douglas E. Kooker)
Aberdeen Proving Ground, MD 21005-5066

National Bureau of Standards
Building 235
ATTN: Henry Prask
Gaithersburg, MD 20899

Commander
ATTN: Code Code G13 (David Dickinson)
Naval Surface Warfare Center
Dahlgren, VA 22448-5000

Internal Distribution:

1510 J. W. Nunziato
1511 D. K. Gartling
1511 R. C. Givler
1511 J. H. Glick (5)
1511 A. M. Kraynik (5)
1512 J. C. Cummings

1512 A. S. Geller(5)
1513 D. W. Larson
1520 L. W. Davison
1530 D. B. Hayes
1550 C. W. Peterson
3141 S. A. Landenberger (5)
3141-1 C. L. Ward (8) for DOE/OSTI
3151 W. I. Klein (3)

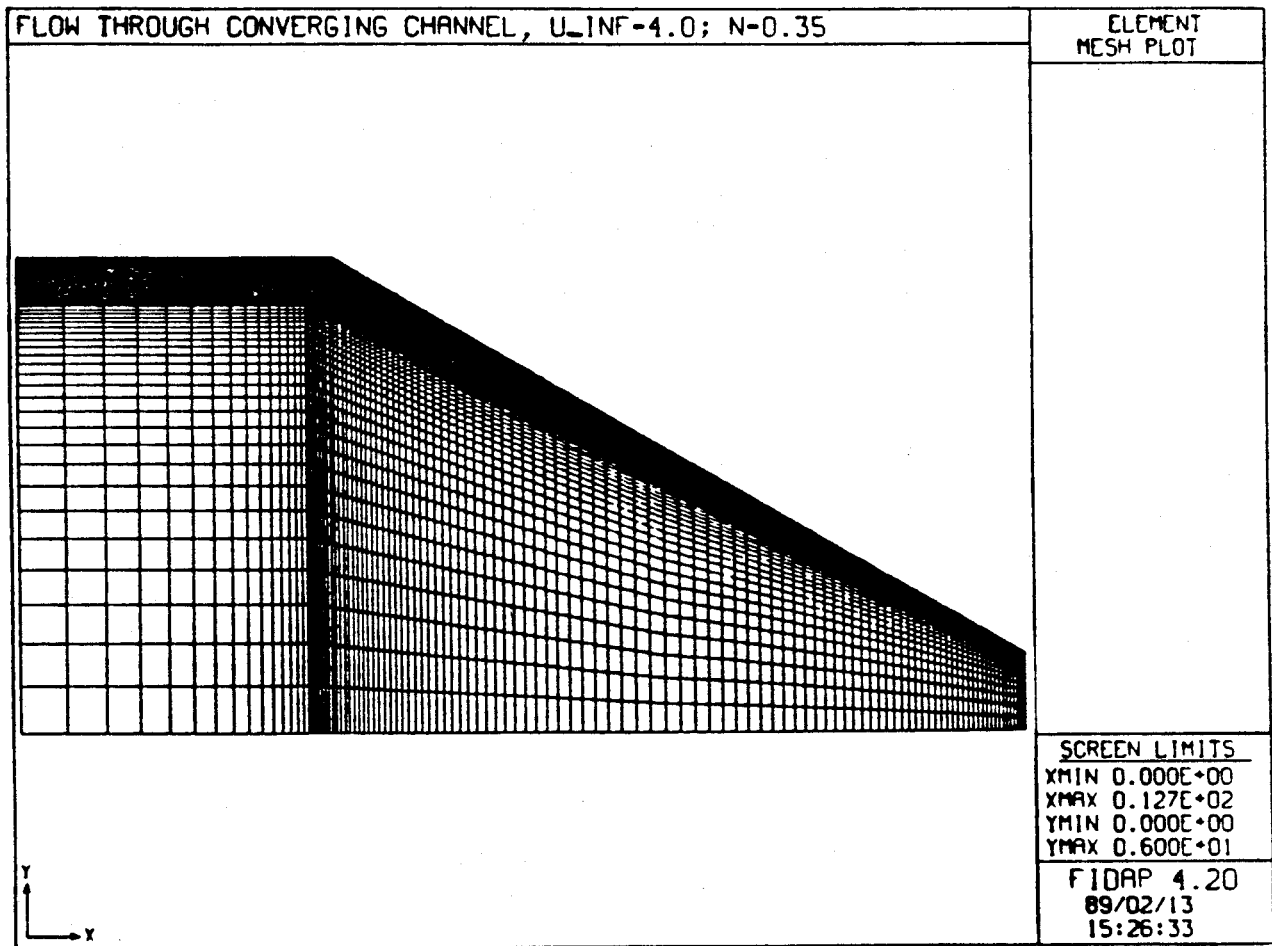


Figure 5: Finite element mesh based on boundary layer analysis